Copy 438
RM L57J14

NACA RM L57J14

NACA

RESEARCH MEMORANDUM

UNCLASSIFIED
By Authority of NASA Tech Pub 7057 Date 10-19-70

PRESSURE MEASUREMENTS ON AN AFTERBODY BEHIND VARIOUS BLUNT NOSE SHAPES AT A MACH NUMBER OF 2

By Katherine C. Speegle

Langley Aeronautical Laboratory
Langley Field, Va.

Declassified by authority of NASA Classification Change Notices No. 209
ed ** 1-30-70

FACILITY FORM 602
N71-70254 (ACCESSION NUMBER)
22 (PAGES)
(NASA CR OR TMX OR AD NUMBER)
(THRU)
(CODE)
(CATEGORY)

NATIONAL ADVISORY COMMITTEE
FOR AERONAUTICS

WASHINGTON

December 27, 1957

NATIONAL ADVISORY COMMITTEE FOR AERONAUTICS

RESEARCH MEMORANDUM

PRESSURE MEASUREMENTS ON AN AFTERBODY BEHIND VARIOUS BLUNT NOSE SHAPES AT A MACH NUMBER OF 2

By Katherine C. Speegle

SUMMARY

An experimental investigation of flow surrounding afterbodies behind blunt nose shapes has been made at a Mach number of 2 and a free-stream Reynolds number based on 1 foot of about 14×10^6 in the 27- by 27-inch preflight jet of the Langley Pilotless Aircraft Research Station at Wallops Island, Va. Pressure measurements were made on and around the afterbodies for each configuration. Pressures are shown to vary only slightly with nose shape. Shadowgraphs of each configuration were made and indicate that separated flow surrounds the entire afterbody for all configurations tested with a wake angle varying from about 5° convergent to 10° divergent.

INTRODUCTION

A blunt nose with a converging afterbody is a shape being considered for the reentry body of long-range ballistic missiles. Extensive tunnel and free-flight tests have been made to determine the flow and heating characteristics of various blunt nose shapes. Little data are available, however, for the afterbody where large regions of separated flow exist. Reference 1 gives limited heating data for such a shape at Mach numbers of 2.0 and 6.9. Chapman, Kuehn, and Larson have made extensive studies of flow-separation phenomena, in which separated regions on forward-facing steps were considered primarily (ref. 2). Investigations in which separated flow behind bodies was considered have been mostly concerned with base drag. A summarization of experimental information and existing methods for predicting base pressures behind bodies of revolution is presented in reference 3.

Prior to conducting free-flight tests to study heating and pressures on the afterbodies behind blunt nose shapes, a preliminary study of the flow pattern around afterbodies has been conducted in the 27- by 27-inch preflight jet of the Langley Pilotless Aircraft Research Station at

Wallops Island, Va. Six blunt noses with the same afterbody configuration were tested at a Mach number of 2.0. The results of these tests as determined by measuring pressures on and making shadowgraphs of the various configurations are presented in this report.

SYMBOLS

M	Mach number
p	pressure, lb/sq in. abs
q	dynamic pressure, lb/sq in.
D	maximum nose diameter, in.
r	radius, in.
T	temperature, ^{o}R
x	afterbody surface distance, in.
l	axial length from nose tip, in.
$\frac{\Delta p}{q}$	pressure coefficient, $\frac{p_l - p_\infty}{q_\infty}$

Subscripts:

l	local
t	total
∞	undisturbed free stream

MODELS AND TESTS

Scaled drawings of the models tested are shown in figure 1. The blunt noses or forebodies had a maximum diameter of 10 inches. The afterbody which approximated a truncated cone had a maximum diameter of 8.39 inches, leaving an 0.8-inch step where the afterbody and forebody were joined. The sixth model was a modification of model A, as shown in figure 1. The models were bodies of revolution constructed of mahogany

in such a manner that the nose shape could be changed and the afterbody would remain fixed to the sting support.

A detailed drawing of the instrumentation of the afterbody is shown in figure 2. A line of seven static-pressure pickups was located on a single ray on the afterbody. Six iron-constantan thermocouples were attached to an Inconel plate 1/32 inch thick and 2 inches wide. The thermocouple ray was located 180° from the pressure orifices.

Tests were made on six different models. During each test, temperatures and static pressures were measured on the afterbody. All models were tested at 0° angle of attack. Model A (fig. 1) was also tested at 5° angle of attack with the pressures and temperatures measured both windward and leeward. Total-pressure probes (fig. 2) were installed in the separated-flow region around the afterbody for model E. Although temperature measurements were made, pressure data only are presented in quantitative form in this report, as is explained in the section entitled "Results and Discussion."

The tests were conducted in the preflight jet facility of the Langley Pilotless Aircraft Research Station at Wallops Island, Va.; the 27- by 27-inch nozzle was used. Photographs of a typical model in test position are shown as figure 3. The tests for a free-stream Mach number of 2 and a free-stream Reynolds number based on 1 foot of about 14×10^6 were at sea-level static-pressure and temperature conditions. The preflight jet is more fully described in reference 4.

Free-stream total pressure and stagnation temperature of the tunnel were measured for each test. The total pressure, 113 pounds per square inch absolute, was obtained by means of a six-cell recording manometer and was the same within 3 percent for all tests. The stagnation temperature measured by thermocouples varied with time and increased slightly as the test proceeded, with a maximum variation from 900° to 980° R for a single test.

The entire model was located within the Mach lines of the jet for all tests, which let the model rest in a free-stream flow field free of any shocks except those originating from the model itself. Measurements presented herein were made after the jet flow had become steady; this condition was reached in about 5 seconds. The air supply was such that constant flow conditions could be maintained for about 6 seconds.

Shadowgraphs were made during the tests for all configurations. The shadowgraph camera was mounted on the right side of the nozzle with the spark source about 30 feet to the left of the model.

RESULTS AND DISCUSSION

Shadowgraphs are shown in figure 4 for each test. The basic observation from these shadowgraphs is the absence of reattachment on the afterbody. Measurements from the shadowgraphs show wake angles from about 5° convergent to 10° divergent. The models were not in contact with the bow-shock—jet-boundary interference which is noted in figure 4(a) and appears in all the shadowgraphs. The configuration in figure 4(a) is shown at 5° angle of attack in figures 4(g) and 4(h). No significant change in the flow pattern is indicated in the shadowgraphs.

Pressure measurements along the surface of the afterbodies are presented in figures 5 and 6 as the ratio of local pressure to measured free-stream total pressure $p_l/p_{t,\infty}$ for all tests. The pressure ratios are plotted as a function of the nondimensional parameter x/D, where x is the distance along the surface from the afterbody-forebody juncture and D is the maximum nose diameter. The measurements from all the pressure orifices remained constant for the entire testing period for all models; therefore, the pressures are presented for only one time after the steady flow and sea-level conditions at Mach number 2 had been reached.

Figure 5 shows the pressure ratio for the five different blunt nose shapes. The accuracy of the pressure-ratio measurements is within ±0.0025. Within this accuracy the afterbody static pressures indicate little pressure change for different forebody shapes with model A having the lowest measured local static pressures and model E having the highest.

Model A (fig. 1) was tested at 5° angle of attack and pressures were measured both windward and leeward. The ratios of local static pressure to free-stream total pressure for model A at angles of attack of 0° and 5° are shown in figure 6. The windward 5° angle-of-attack measurements are slightly lower than the 0° angle-of-attack measurements; this signifies that the flow on the windward side of the afterbody is accelerated but still separated. Likewise the leeward measurements indicate a small deceleration of the flow.

Figure 6 also shows the pressure ratios for model A modified as shown in figure 1(a). The pressures were lower for the rounded corner, but the afterbody again remains completely within the separated flow region.

Four total-pressure measurements were made in the area surrounding the afterbody for model E. (See fig. 2.) Two of the probes were 90° from the static-pressure orifices and were located 1 inch behind the step at a vertical distance of 0.44 and 0.88 inch from the surface. The other two probes were 270° from the afterbody-static-pressure orifices

ray and were located 4 inches behind the step at a vertical distance of 0.96 and 1.92 inches from the surface. The pressures measured by the total-pressure probes and measured afterbody local pressures are shown in figure 7 along with the location of each measuring station. The pressures are equal for all stations and the same as those measured on the afterbody, further indicating the existing dead-air region.

Pressure coefficients $\Delta p/q$ on the afterbodies of the five nose shapes are presented in figure 8. Also shown is a base pressure coefficient for a cylindrical body of revolution from reference 3. Reference 5 gives the effects of sting-support interference on base pressures for bodies of revolution. This information is also shown in figure 8. The measured pressure coefficients are less than the base pressure coefficients predicted by reference 3 but are close to the predictions of reference 5. This indicates that the afterbodies may be acting the same as a large sting behind the blunt noses.

Temperature measurements were made on the afterbody in the manner described in the section entitled "Models and Tests." The heat-transfer coefficients calculated from the measured temperatures showed a variation with time which was greater than could be estimated because of losses through conduction, radiation, and so forth. Therefore, these measurements were not considered of a quality suitable for presentation in quantitative form.

Qualitatively the measurements appeared to agree favorably with the afterbody heating presented in reference 1.

CONCLUDING REMARKS

Pressures were measured on and around afterbodies behind various blunt nose shapes at a Mach number of 2 and a Reynolds number based on 1 foot of about 14×10^6. The variation of the shape of blunt noses had little effect on the afterbody pressures. These pressure measurements along with the shadowgraphs indicate that the separated-flow region completely surrounds the afterbodies for all blunt nose shapes tested for both 0° and 5° angle of attack. The wake angle varies approximately 5° convergent to 10° divergent. The pressure coefficients (measured on the

afterbodies) can be approximated by base pressure coefficients corrected for the effect of a sting as given in University of Illinois ME Technical Note 392-2.

Langley Aeronautical Laboratory,
National Advisory Committee for Aeronautics,
Langley Field, Va., September 27, 1957.

REFERENCES

1. Crawford, Davis H., and Rumsey, Charles B.: Heat Transfer in Regions of Separated and Reattached Flows. NACA RM L57D25b, 1957.

2. Chapman, Dean R., Kuehn, Donald M., and Larson, Howard K.: Investigation of Separated Flows in Supersonic and Subsonic Streams With Emphasis on the Effect of Transition. NACA TN 3869, 1957.

3. Love, Eugene S.: Base Pressure at Supersonic Speeds on Two-Dimensional Airfoils and on Bodies of Revolution With and Without Fins Having Turbulent Boundary Layers. NACA TN 3819, 1957. (Supersedes NACA RM L53C02.)

4. Faget, Maxime A., Watson, Raymond S., and Bartlett, Walter A., Jr.: Free-Jet Tests of a 6.5-Inch-Diameter Ram-Jet Engine at Mach Numbers of 1.81 and 2.00. NACA RM L50L06, 1951.

5. Korst, H. H., Page, R. H., and Childs, M. E.: A Theory for Base Pressures in Transonic and Supersonic Flow. ME Tech. Note 392-2 (Contract No. AF 18(600)-392), Univ. of Illinois, Eng. Exp. Station, Mar. 1955.

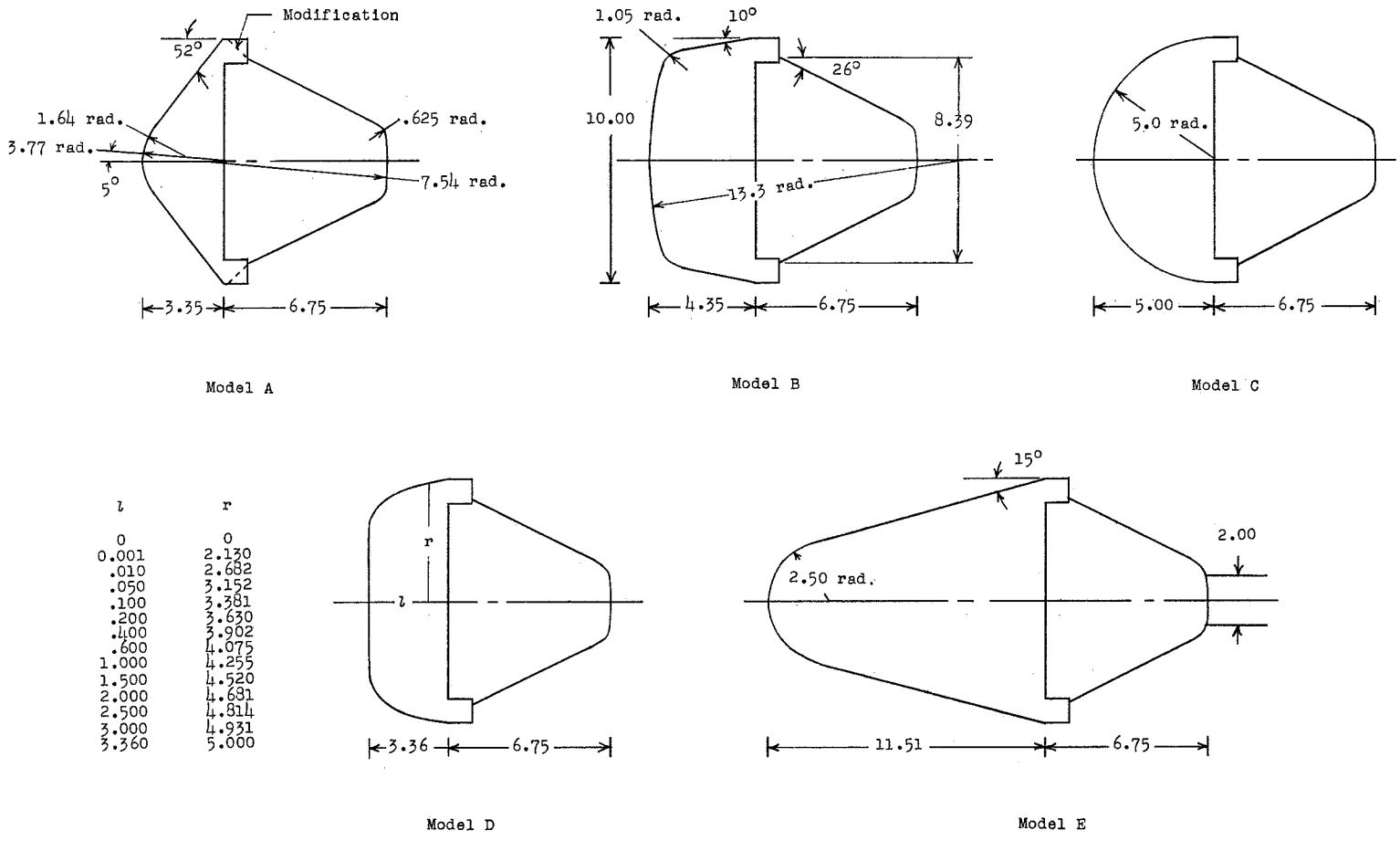

Figure 1.- Model configurations used in tests. All dimensions are in inches unless otherwise indicated.

Pressure orfice	Distance from nose-afterbody juncture
1	0.56
2	1.11
3	2.23
4	3.34
5	4.45
6	5.56
7	6.12
Thermocouple	
1	0.50
2	1.25
3	2.00
4	3.00
5	4.00
6	5.00

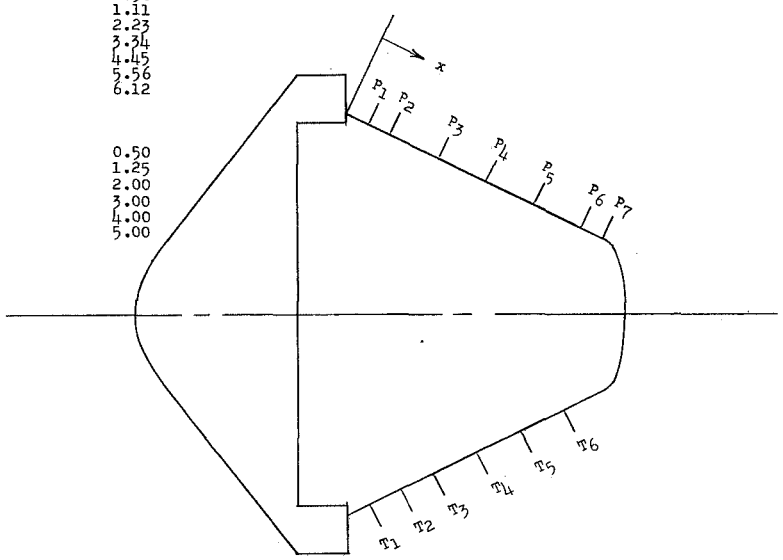

(a) Surface pressure and temperature pickup locations.

Total pressure	Vertical distance from afterbody surface
1	0.44
2	.88
3	.96
4	1.92

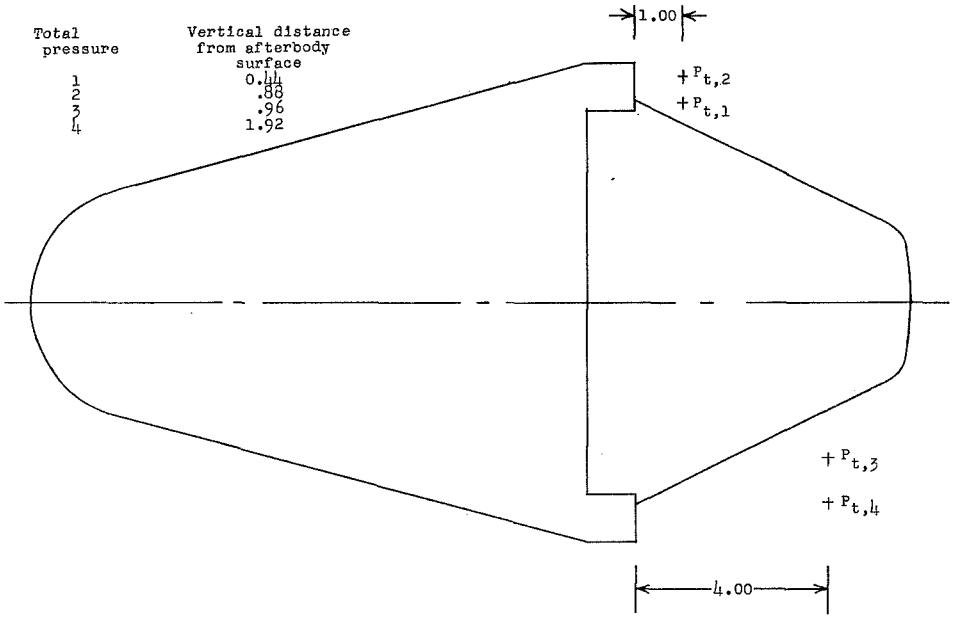

(b) Total-pressure probe locations used for model E only. Sketch is rotated 90° from sketch in figure 2(a).

Figure 2.- Afterbody instrumentation. All dimensions are in inches.

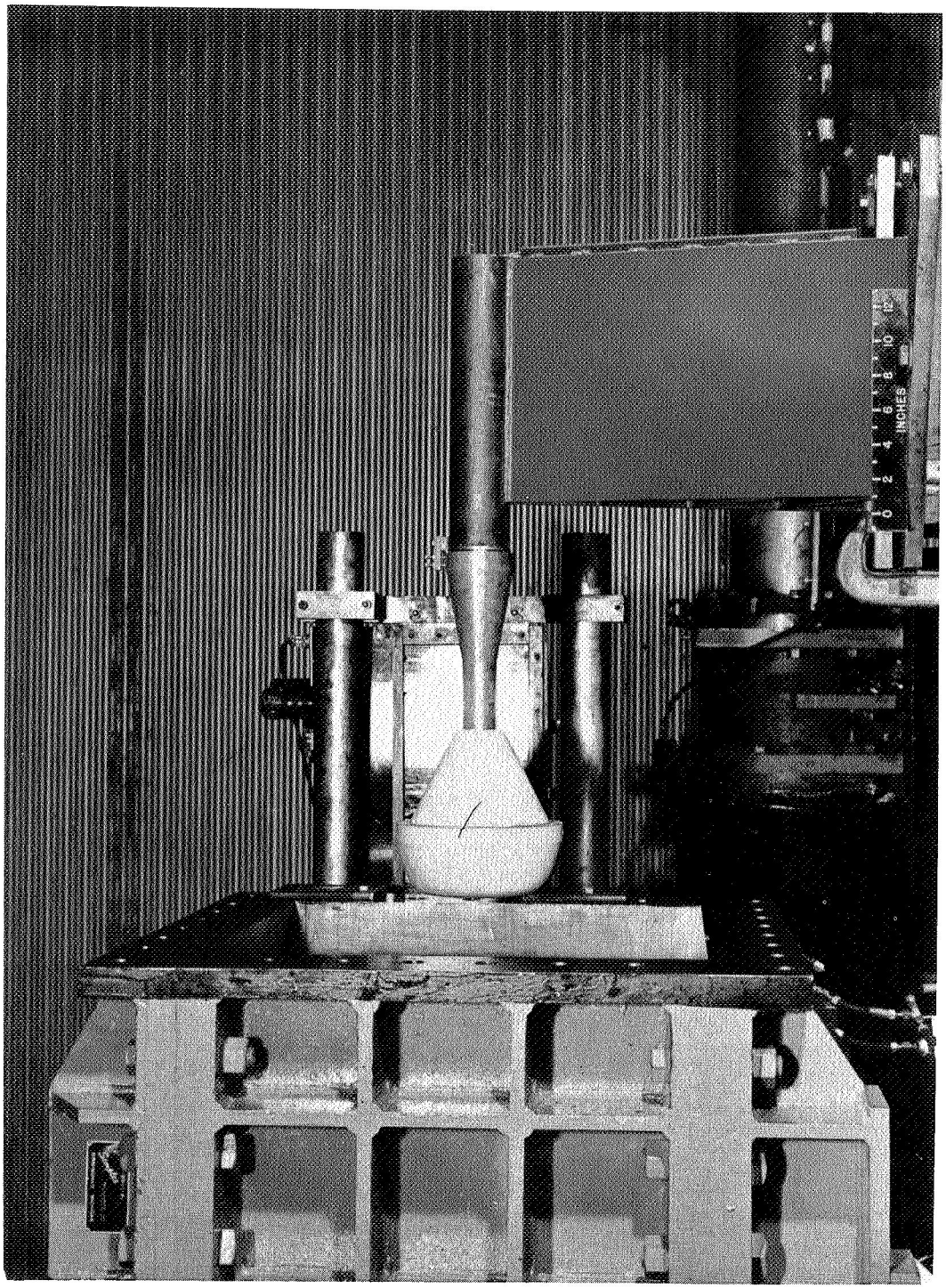

Figure 3.- A typical model in testing position. L-57-2010.1

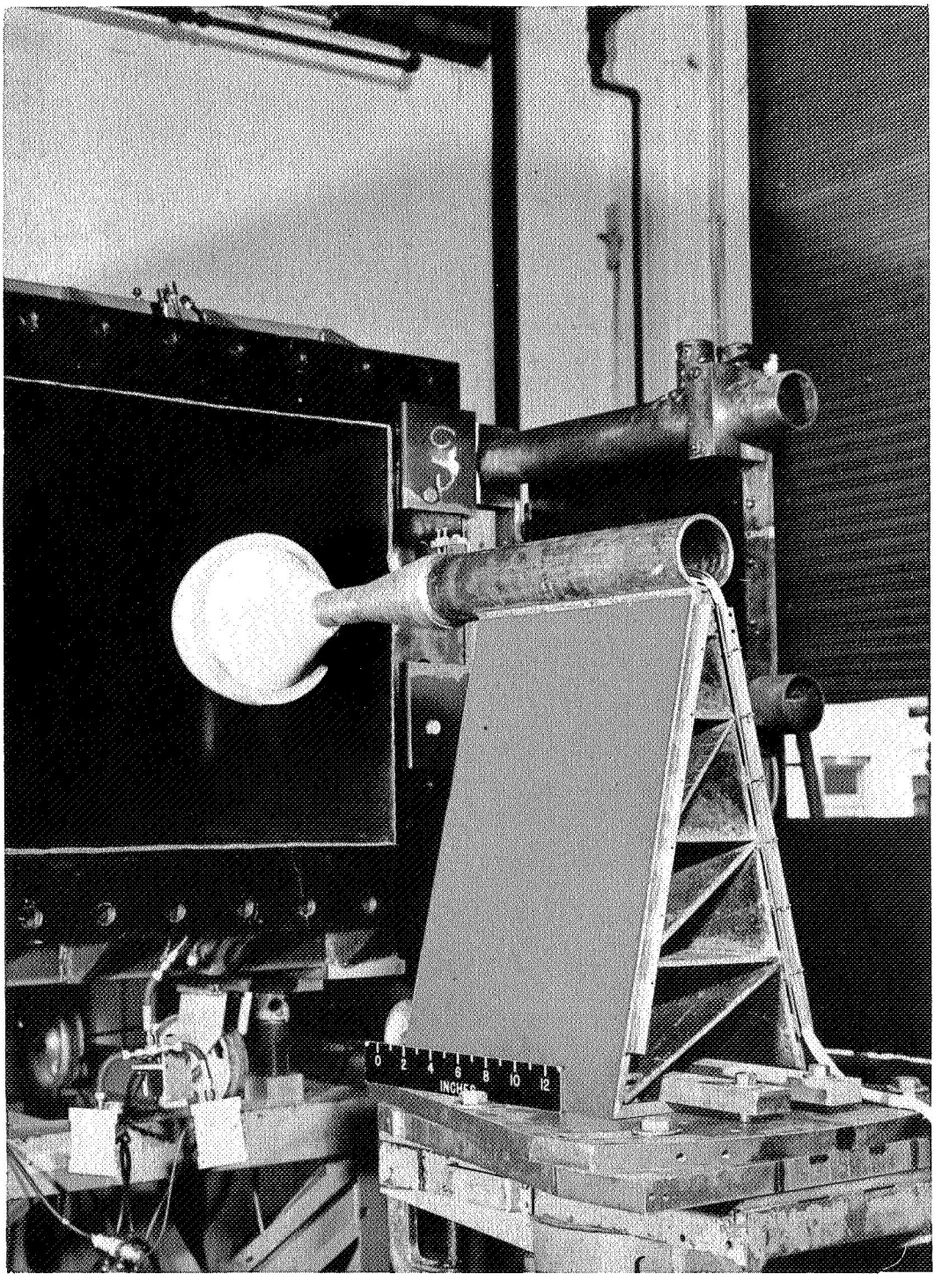

Figure 3.- Concluded. L-57-2011.1

(a) Model A. L-57-2766

Figure 4.- Shadowgraphs of tested configurations.

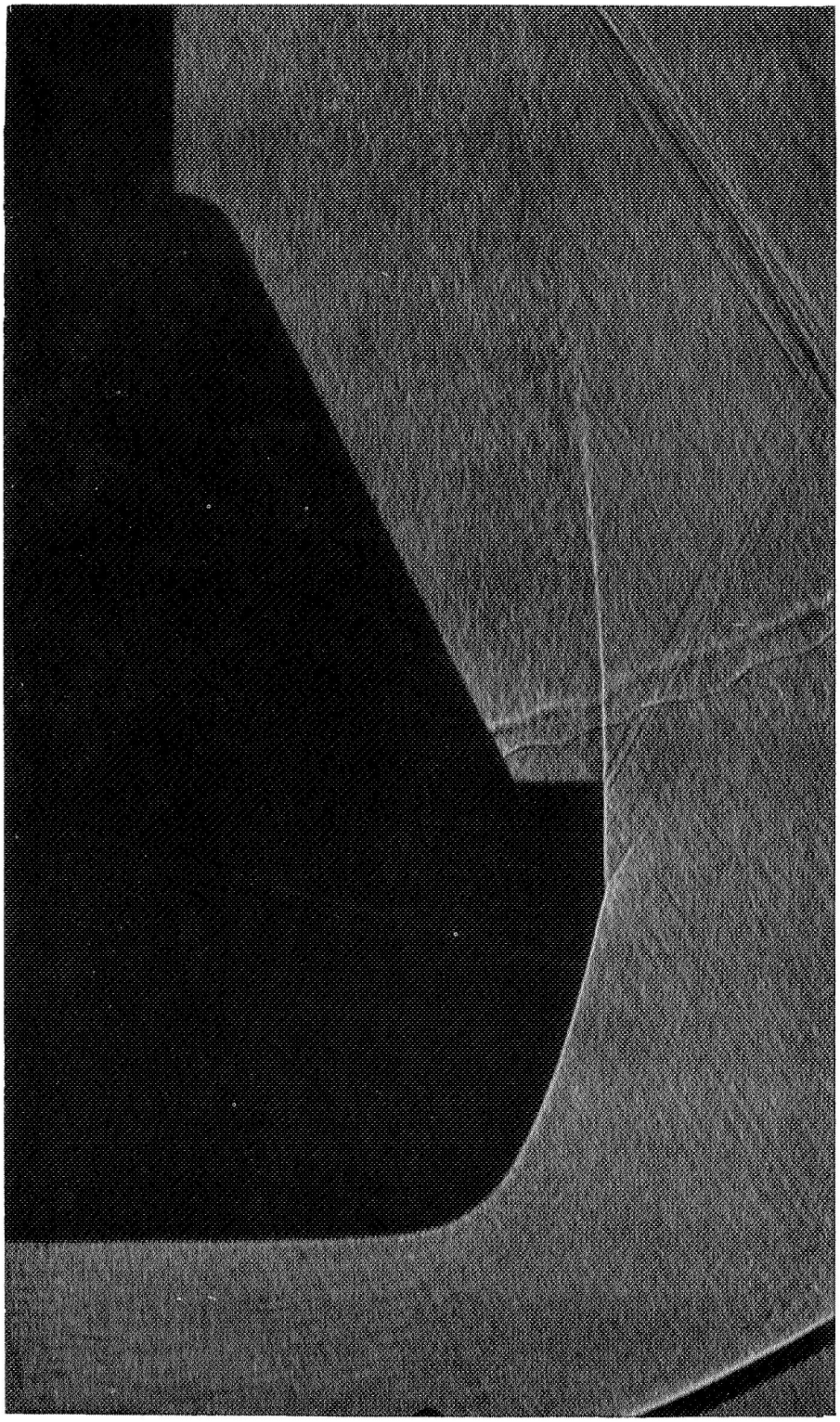

(b) Model B. L-57-2767

Figure 4.- Continued.

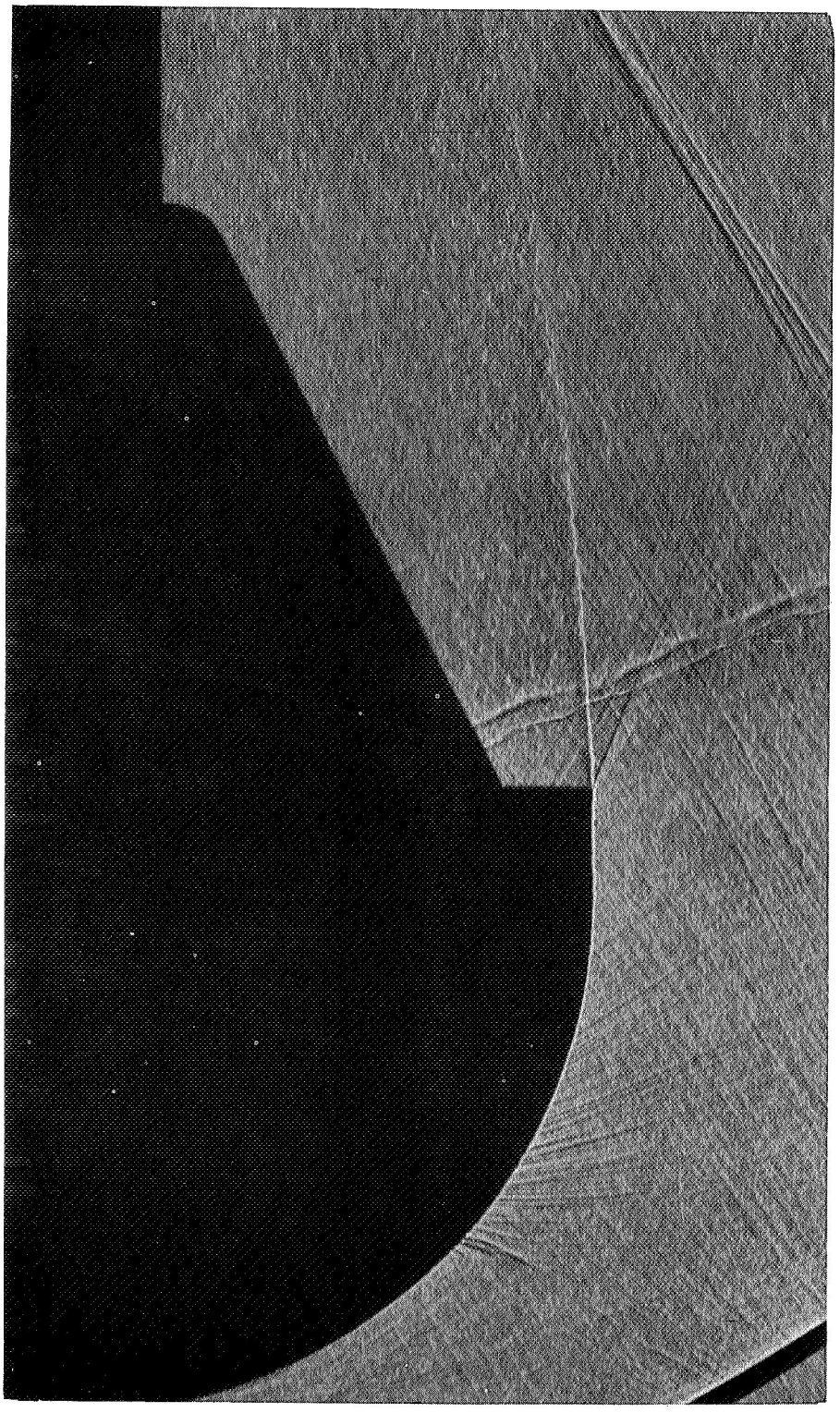

(c) Model C. L-57-2768

Figure 4.- Continued.

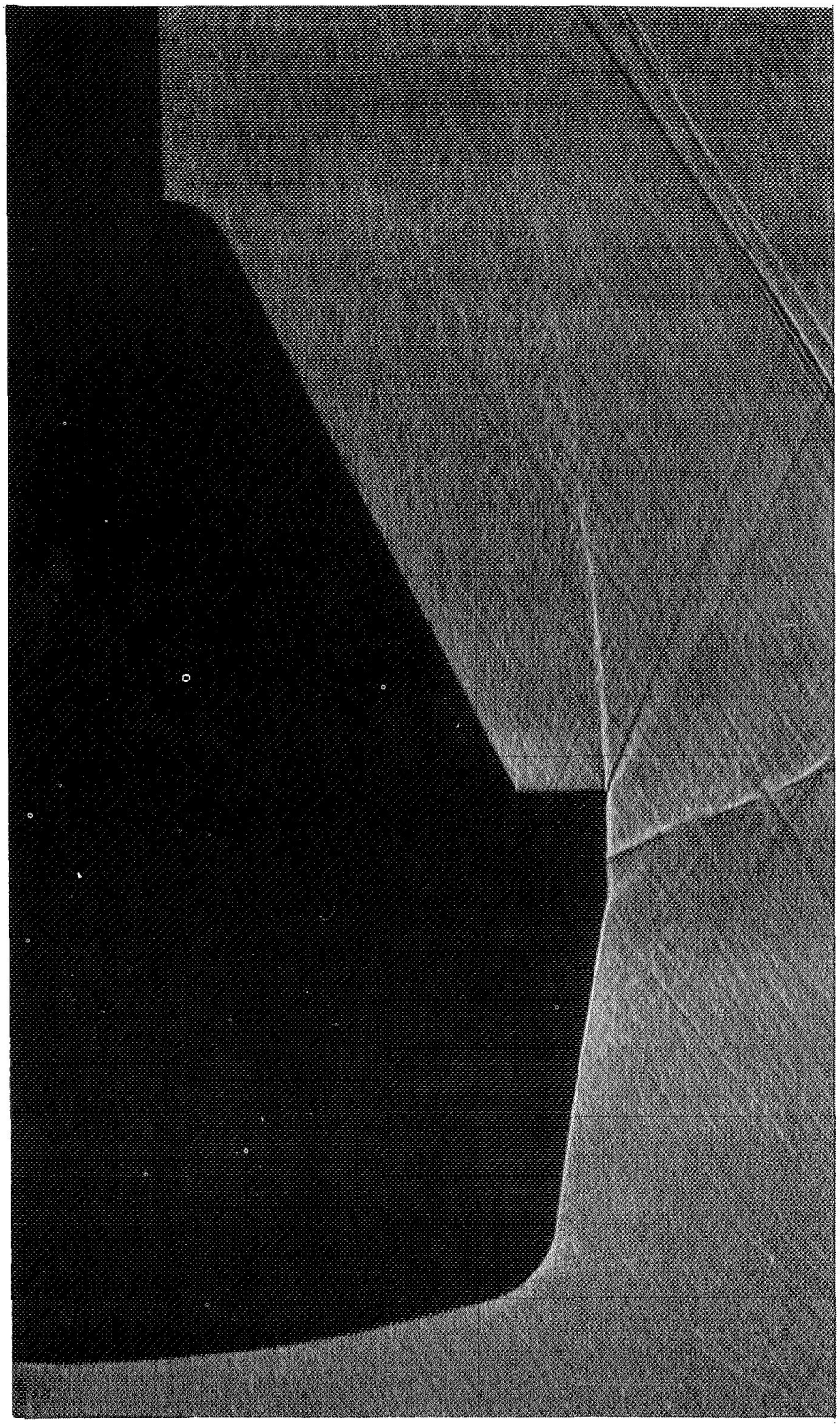

(d) Model D. L-57-2769

Figure 4.- Continued.

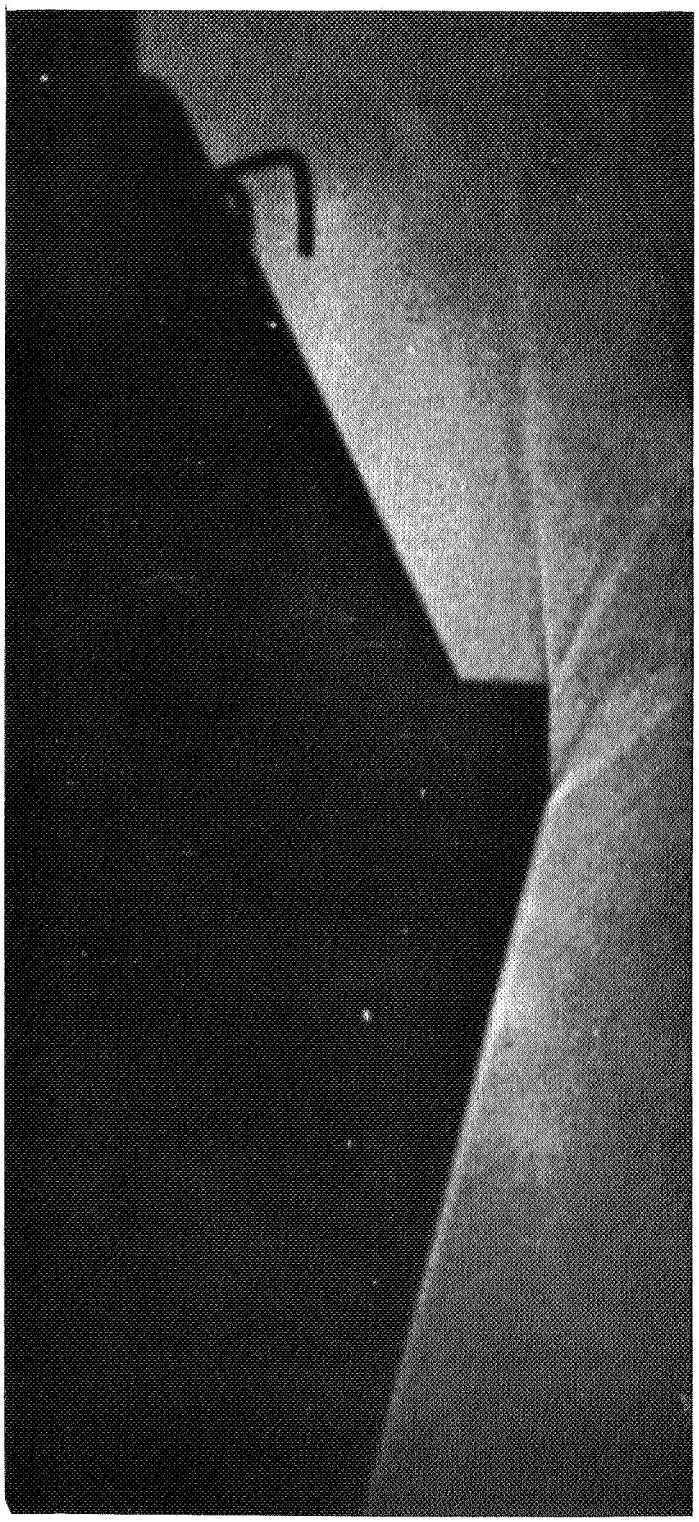

L-57-2770

(e) Model E.

Figure 4.- Continued.

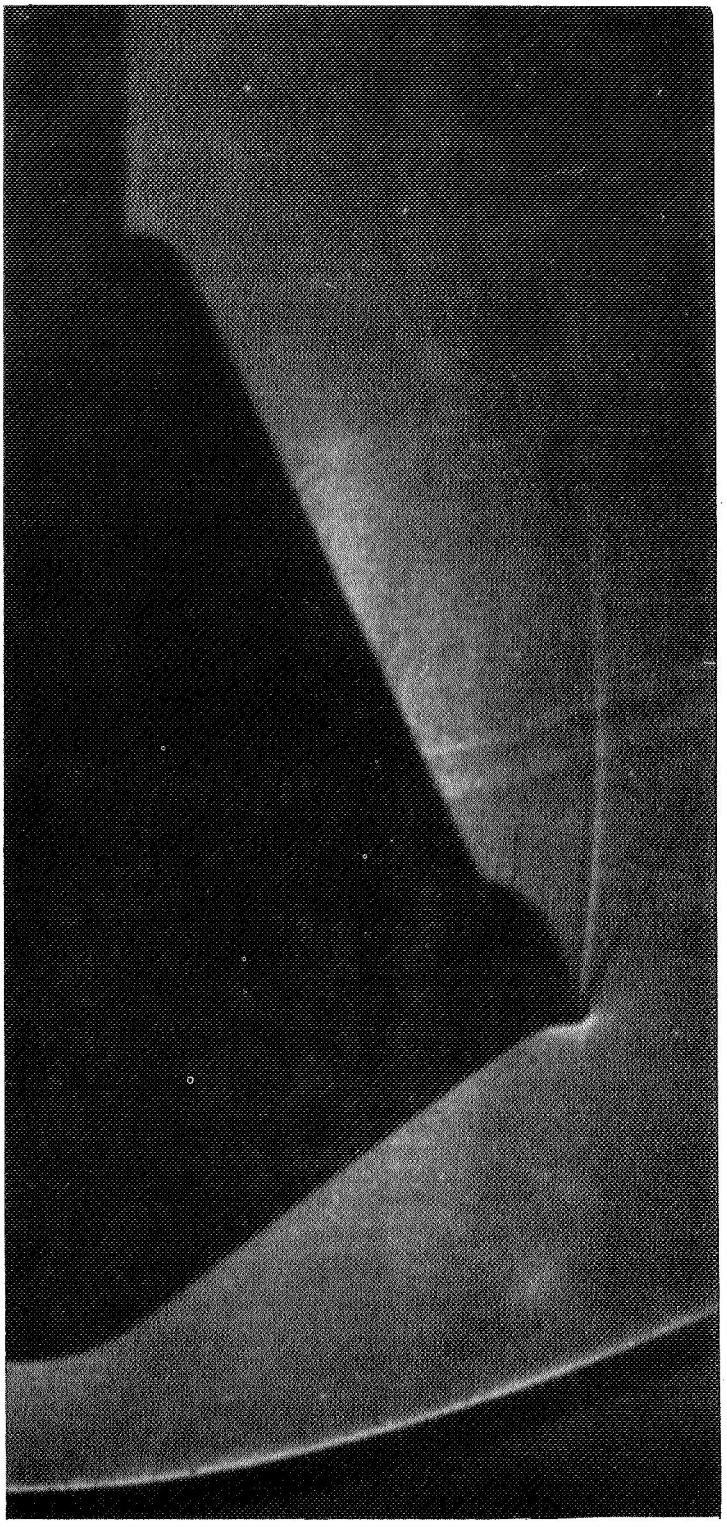

(f) Model A modified. L-57-2771

Figure 4.- Continued.

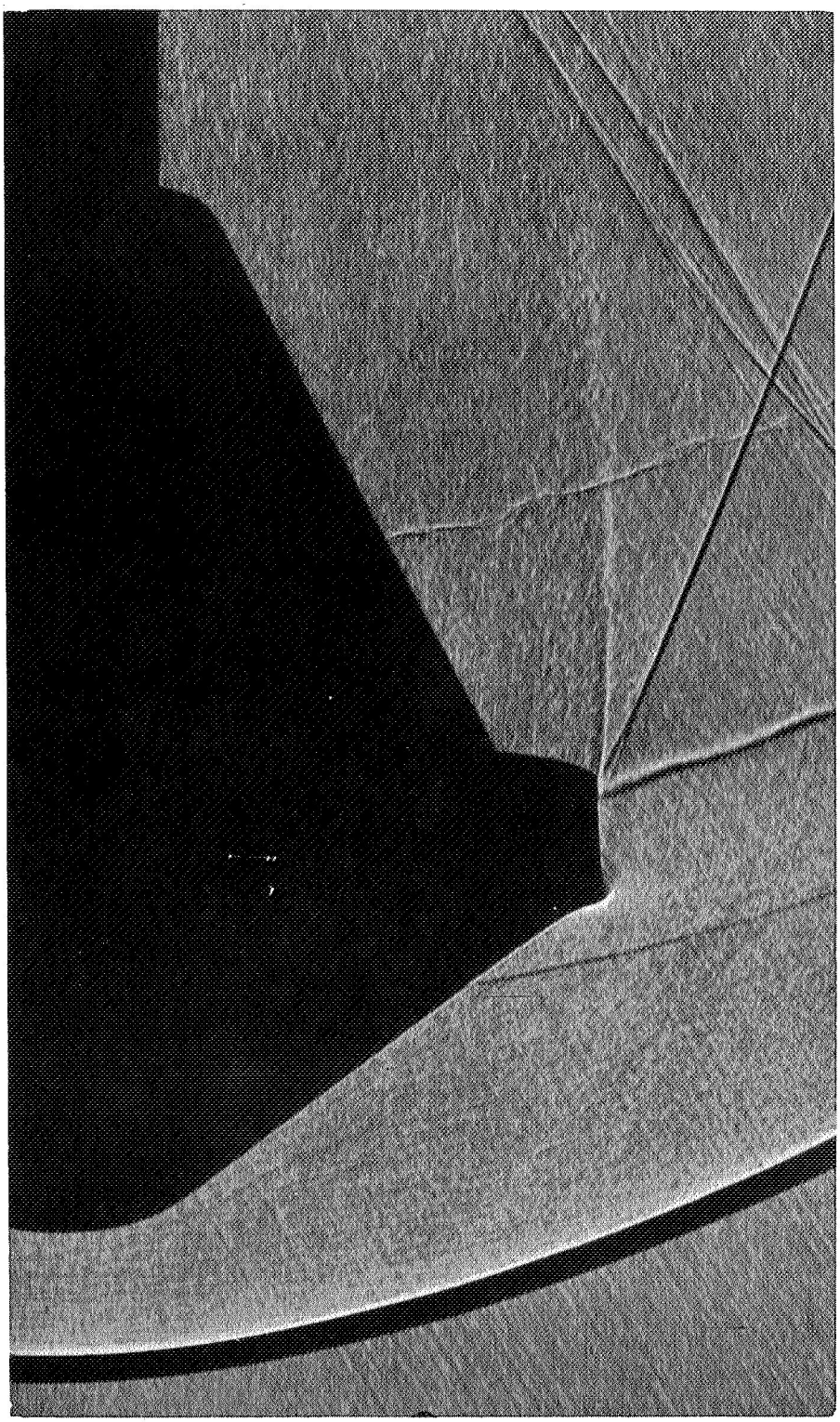

(g) Model A at 5° angle-of-attach, leeward. L-57-2772

Figure 4.- Continued.

(h) Model A at 5° angle-of-attach, windward. L-57-2773

Figure 4.- Concluded.

CONFIDENTIAL

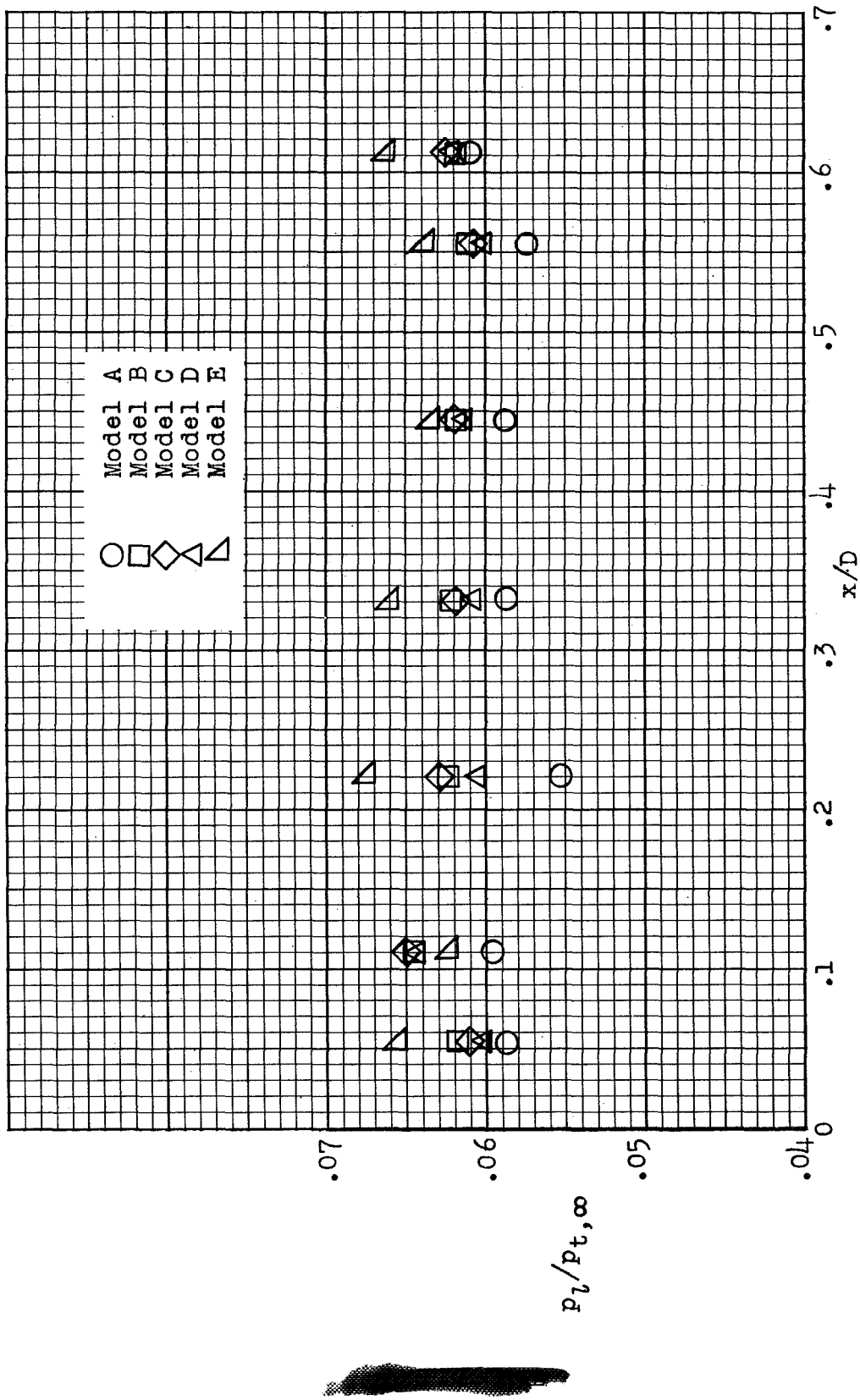

Figure 5.- Ratio of local static pressure to free-stream total pressure for varying nose shape.

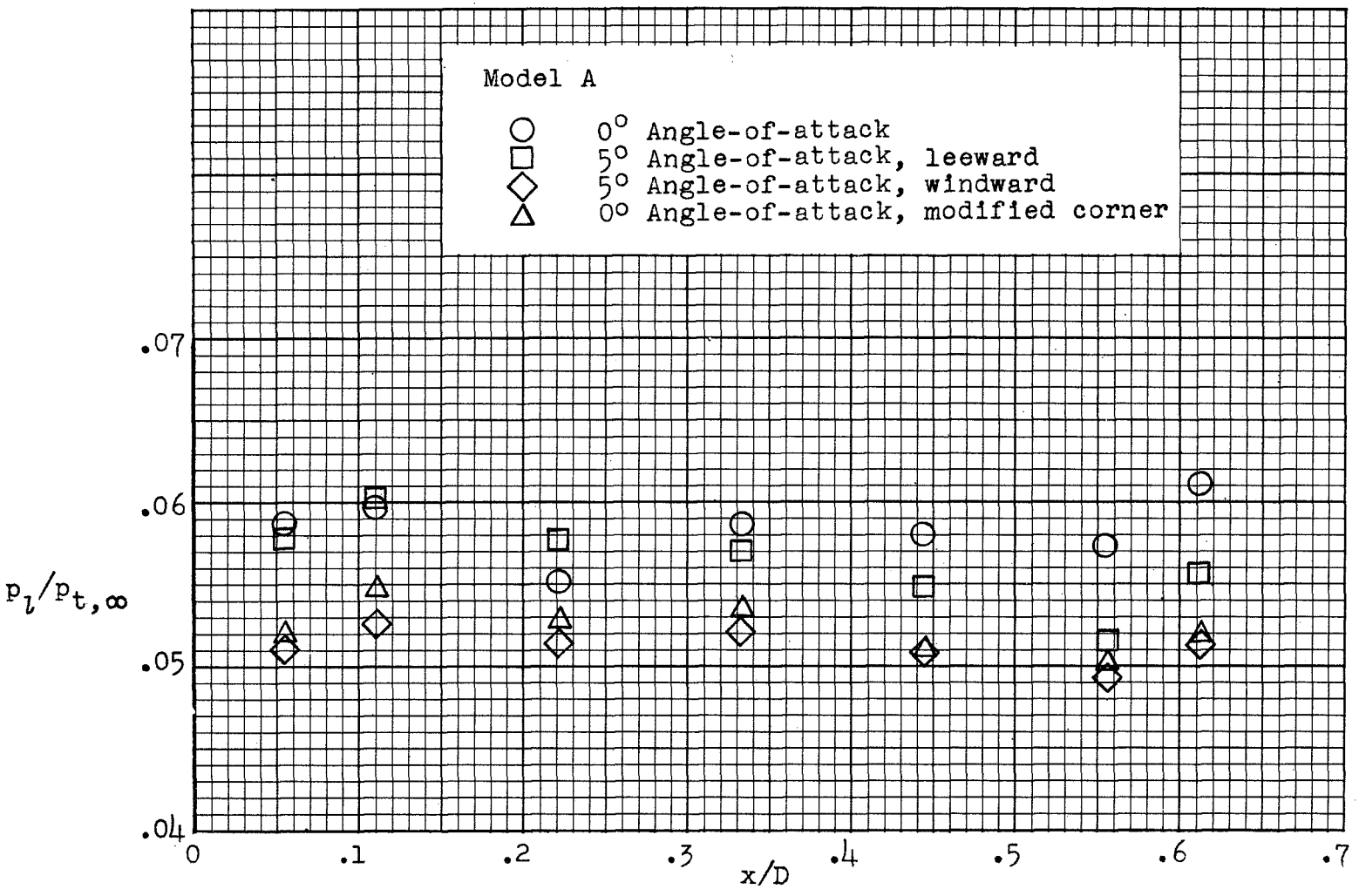

Figure 6.- Ratio of local static pressure to free-stream total pressure for model A at angle of attack and for model A modified.

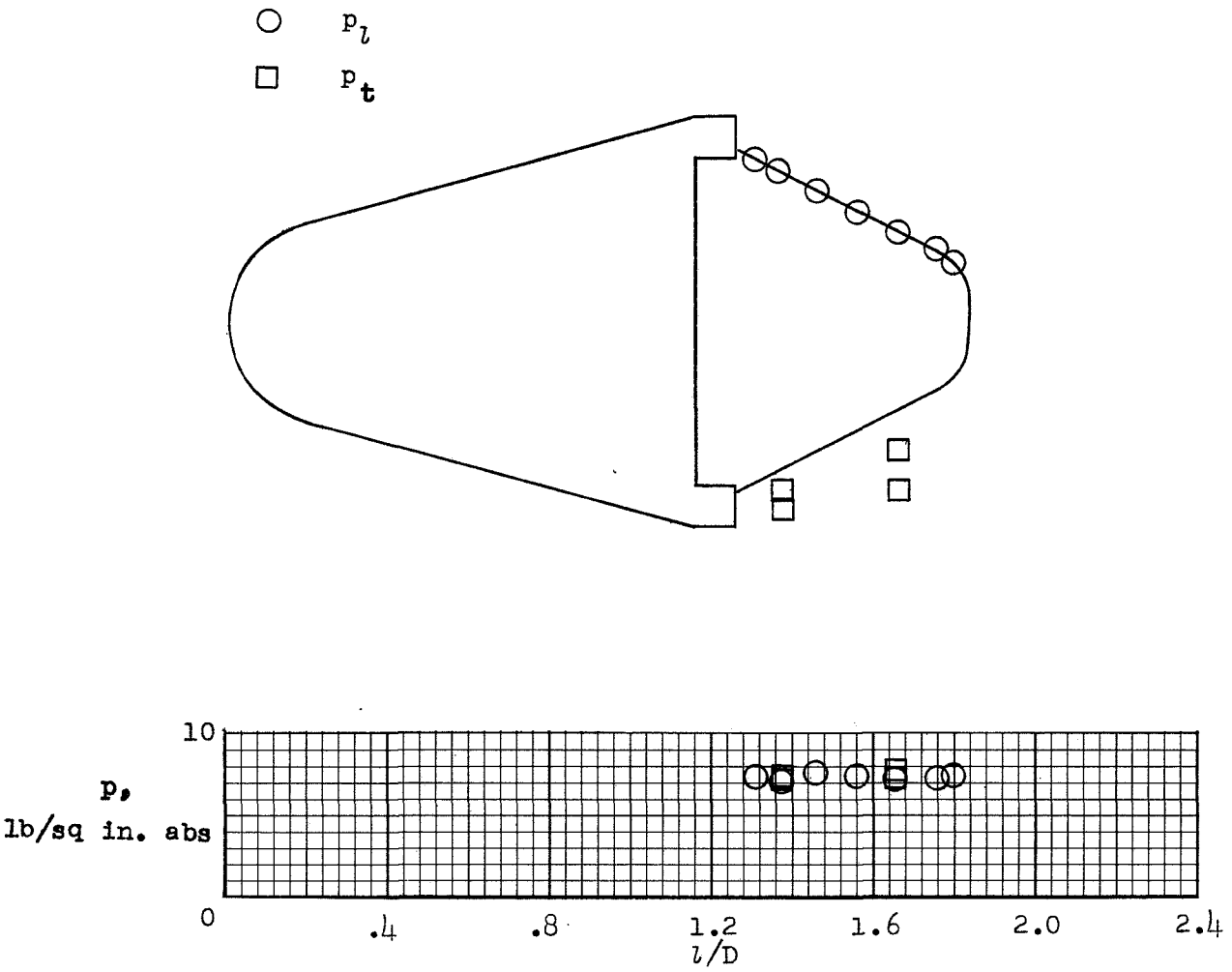

Figure 7.- Locations and measurements of pressures on the afterbody and in the region around the afterbody for model E, where free-stream total pressure equals 115.795 pounds per square inch absolute.

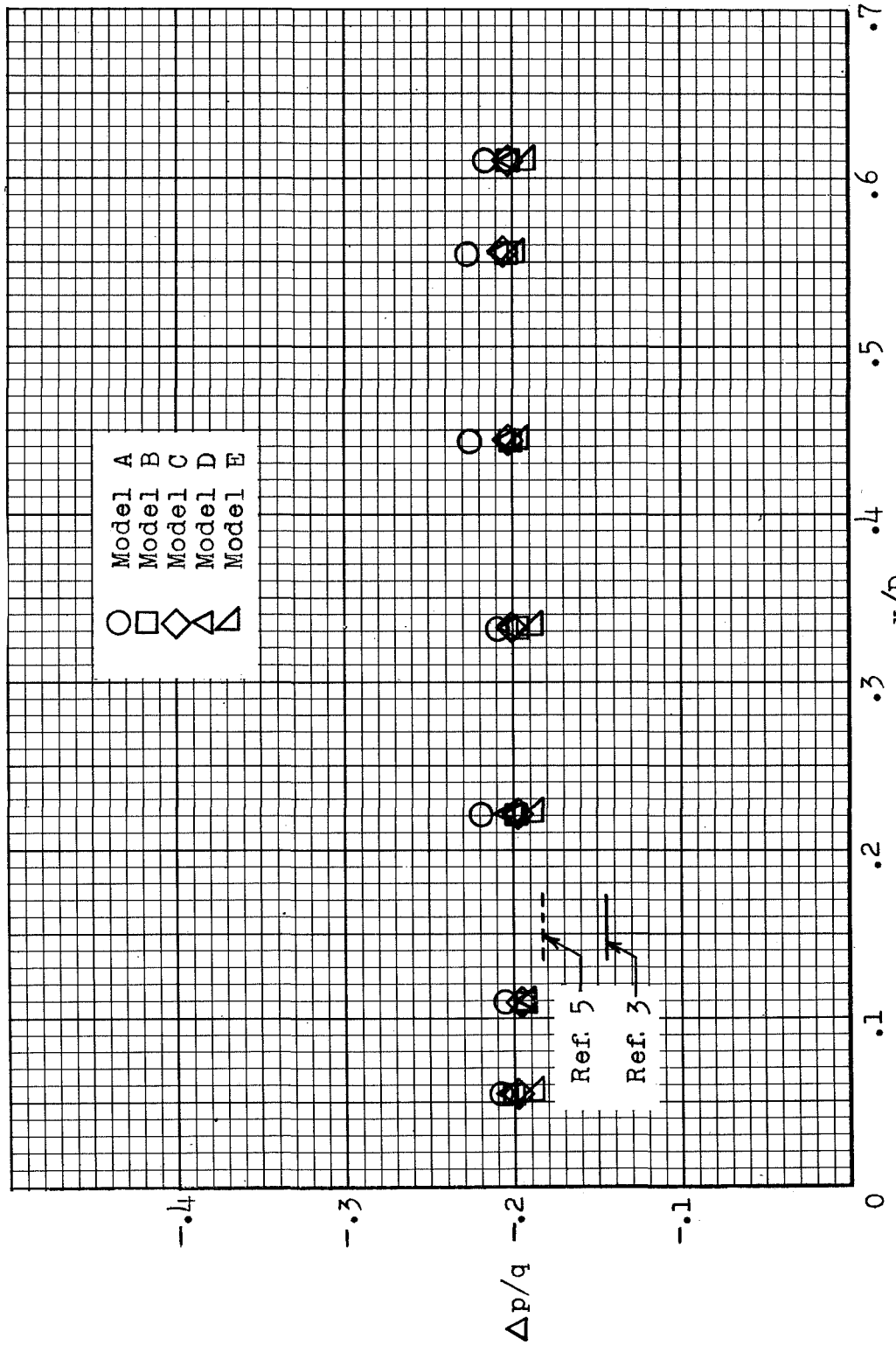

Figure 8.- Pressure coefficients on the afterbody for various nose shapes.